

## **Auroral physics at Jupiter: Outstanding issues to be addressed by Juno**

**W. S. Kurth** (1), J. E. P. Connerney (2), D. J. McComas (3,4), B. H. Mauk (5), R. Gladstone (3), A. Adriani (6), F. Bagenal (7), and S. J. Bolton (3)

(1) University of Iowa, Iowa City, Iowa, (2) NASA/Goddard Space Flight Center, Greenbelt, Maryland, (3) Southwest Research Inst., San Antonio, Texas, (4) University of Texas, San Antonio, Texas, (5) Applied Physics Laboratory, Johns Hopkins University, Laurel, Maryland, (6) Inst. for Space Astrophysics and Planetology, Rome, Italy, (7) University of Colorado, Boulder, Colorado. (william-kurth@uiowa.edu / Fax: 319 3351753)

### **Abstract**

Juno is on course to enter polar orbit at Jupiter on July 4, 2016. After a small number of preliminary orbits during which the orbital period is reduced, approximately 30 science orbits will be executed to explore the interior of Jupiter, hence, its origin. A second primary objective of the mission, and the subject of this talk, is to carry out the first exploration of Jupiter's polar magnetosphere with an emphasis on the physics of the Jovian aurora. All previous missions to Jupiter, including Ulysses, remained at low Jovian latitudes at close range, hence, our knowledge of Jupiter's polar magnetosphere and, in particular auroral processes, is a composite of remote sensing (such as radio emissions in the hectometric and decametric bands as well as IR and UV images); application of observations of Earth's auroral and polar cap particles, fields, and auroral emissions; and modeling. While these likely inform our expectations of what Juno will actually measure qualitatively, Juno will provide the first in depth exploration of auroral processes at another planet, other than a small number of very brief encounters of Saturn's kilometric radio source region by Cassini. With a reasonably complete suite of in situ magnetospheric measurements coupled with remote sensing, Juno will enable us to compare the physics of Jupiter's polar magnetosphere with those expectations. Certainly, understanding the nature of auroral currents and mechanisms for particle acceleration are high on the list of priorities for these studies. In addition, it is expected that Juno will greatly improve our understanding of the mapping of auroral processes from high latitudes and low altitudes to the middle and outer magnetosphere.

## Zebra spectral structures in Jovian decametric radio emissions

S. Rošker (1), M. Panchenko (2), H.O. Rucker (1), A.I. Brazhenko (3)

(1) Commission for Astronomy, Austrian Academy of Sciences, Graz, Austria (helmut.rucker@oeaw.ac.at)

(2) Space Research Institute, Austrian Academy of Sciences, Graz, Austria

(3) Radioastronomical Institute Poltava, National Academy of the Ukraine, Poltava, Ukraine

### Abstract

Jupiter with the largest planetary magnetosphere in the solar system emits intense coherent non-thermal radiation in a wide frequency range. This emission is a result of complicated interactions between the dynamic Jovian magnetosphere and energetic particles supplying free energy from planetary rotation and the interaction between Jupiter and the Galilean moon Io. Decametric radio emission (DAM) is the strongest component of Jovian radiation observed in a frequency range from a few MHz up to 40 MHz. Depending on the time scales the Jovian DAM exhibits different complex spectral structures.

Recent observations of the Jovian decametric radio emission using the large ground-based radio telescope URAN-2 (Poltava, Ukraine) enabled the detection of fine spectral structures, specifically zebra stripe-like patterns, never reported before in the Jovian decametric wavelength regime (Figure 1).

In this presentation we describe and analyse these new observations by investigating the characteristics of the Jovian decametric zebra patterns. On basis of these findings the possible mechanism of wave generation is discussed and in particular the value of the determination of local plasma densities within the Jovian magnetosphere by remote radio sensing is emphasized.

### 1. Analysis of observations of zebra patterns in Jovian decametric radio emission

The data used for the present study are from observations of the radio telescope URAN-2 (Poltava, Ukraine), one of the largest low frequency telescopes in Europe, operated in the decametric frequency range and equipped with high performance digital radio spectrometers. The antenna array of URAN-2 consists of 512 crossed dipoles with an effective area of

28000 m<sup>2</sup> and beam pattern size of 3.5 x 7 deg at 25 MHz [1]. The instrument enables continuous observations of the Jovian radio emission during long periods of time (depending on Jupiter visibility) with relatively high time-frequency resolution (4 kHz, 100 ms) in the broad frequency range (8-32 MHz). Using the large ground-based radio telescope URAN-2 49 events of stripe-like zebra patterns have been observed within the period September 2012 through March 2015 in the frequency range 15 – 25 MHz which correspond to potential radio sources at 0.25 – 0.05 R<sub>J</sub> above the Jupiter 1 bar level [9]. The structure in the dynamic spectra is similar to those observed from the Sun [2, 3, 4] and suggests a similar generation mechanism, the Double Plasma Resonance (DPR).

A recent study reported on zebra pattern in low-frequency (tens of kHz) Jovian radio emission, observed by Cassini during the Jupiter flyby 2000/2001 (Kuznetsov et al. (2013) and references therein). On basis of the available URAN-2 observations of zebra patterns in the MHz-range detailed investigations are performed with the aim to fully characterize these stripe-like fine structures (Figure 1) under the following aspects:

- a) Occurrence of zebra patterns in dependence of CML (Central Meridian Longitude of Jupiter) and Io phase
- b) Frequency range of occurrence of zebra pattern within the observable range of 15 - 25 MHz
- c) Modulation in frequency, frequency bandwidth of individual zebra pattern ( $f_{min}$ ,  $f_{max}$ )
- d) Modulation length in time (duration of zebra pattern and “wavelength” of modulation)
- e) Modulation depth in intensity
- f) Splitting distance ( $\Delta f$ ) between frequency-varying stripes

g) Determination of polarization (indication of Jovian hemispheric source location)

These investigations visualize some general characteristics or even categories of zebra patterns on which a current model scenario can be proven or even improved.

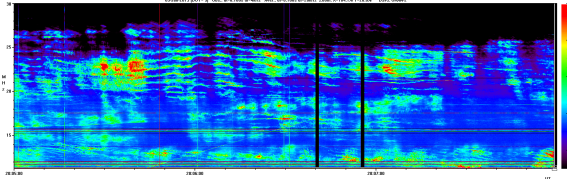


Figure 1: Dynamic spectrum of Jovian decametric radio emission observed on Jan 05, 2013, by the URAN-2 radio telescope (Poltava, Ukraine). Zebra stripe-like patterns occur in the frequency range between 20 MHz and 25 MHz.

## 2. Investigation of Double Plasma Resonance (DPR) and discussion of results

Stripe-like spectral structures or zebra patterns were first observed in the radio spectra of the Sun as quasi-harmonical stripes. The origin of this emission was suggested to be located in the magnetic loops containing energetic particles which produce the plasma waves generated close to the upper-hybrid frequency. The intensity of these waves is significantly higher in the regions where the local upper hybrid frequency equals the harmonics of the local gyrofrequency of the electrons. This mechanism is known as the Double Plasma Resonance (DPR) [6, 7, 10]. These plasma (upper hybrid) waves are transformed into electromagnetic radio waves due to nonlinear processes and can escape the solar magnetic loops. This theory of generation of the zebra patterns in solar radio spectra is well developed and fits the observations [4].

During its Jupiter flyby 2000/2001 Cassini RPWS (Radio and Plasma Wave Science experiment) registered complex striped spectral structures in the Jovian broad-band kilometric radiation at frequency ranges 30-70 kHz [5]. Recently Kuznetsov and Vlasov (2013) have shown that Cassini RPWS observations of modulated low radio frequencies (tens of kHz) are very similar to the zebra patterns detected in the solar radio spectra at decametric frequencies (tens of MHz). The DPR is supposed to occur in a weakly anisotropic

magnetoplasma, where the plasma frequency  $f_p$  exceeds the cyclotron frequency  $f_c$ :  $f_p \gg f_c$ . The generation efficiency of the plasma waves is significantly high if their frequency (close to the upper hybrid frequency  $f_{uh}$ ) is at the harmonics of the electron cyclotron frequency  $f_c$ :  $f_{uh} \cong s * f_c$  with  $s = 2, 3, 4 \dots$ . Based on these findings the investigations of the Jovian dynamic spectra in the decametric frequency range unprecedentedly enable the determination of local plasma density in the vicinity of Jupiter by remote radio sensing.

## Acknowledgements

We would like to acknowledge support from the Austrian Academy of Sciences and we thank the Radioastronomical Team under the lead of Prof. Konovalenko of the Institute of Radioastronomy of the National Academy of the Ukraine for providing corresponding data from Jovian DAM emission.

## References

- [1] Brazhenko, A. I. et al., New decameter radiopolarimeter URAN-2, *Kinematika i Fizika Nebesnykh Tel Suppl.* 5, 43, 2005.
- [2] Chen, B., Bastian, T.S., Gary, D.E., Jing, J., Spatially and spectrally resolved observations of a zebra pattern in a solar decametric radio burst, *Astrophys. J.* 736, 64, 1105.0715, 2011.
- [3] Chernov, G.P., Solar radio bursts with drifting stripes in emission and absorption, *Space Sci. Rev.* 127, 195-326, 2006.
- [4] Chernov, G.P., Recent results of zebra patterns in solar radio bursts. *Research in Astronomy and Astrophysics* 10, 821–866, 2010.
- [5] Kurth, W.S., G.B. Hospodarsky, D.A. Gurnett, A. Lecacheux, P. Zarka, M.D. Desch, M.L. Kaiser, W.M. Farrell, High-resolution observations of low-frequency Jovian radio emissions by Cassini, in: *Planetary Radio Emissions V*, H.O. Rucker, M.L. Kaiser, Y. Leblanc (eds.), Austrian Academy of Sciences Press, Vienna, p.15, 2001.
- [6] Kuijpers, J., A unified explanation of solar type IV DM continua and zebra patterns. *Astron. & Astrophys.* 40, 405 - 410, 1975.
- [7] Kuznetsov, A.A., Y.T. Tsap, Loss-cone instability and formation of zebra patterns in Type IV solar radio bursts. *Solar Phys.* 241, 127–143, 2007.

- [8] Kuznetsov, A.A., V.G. Vlasov, Formation of zebra pattern in low-frequency Jovian radio emission, Planet. Space Sci., arXiv: 1209.2923v1 [astro-ph.EP], 2013.
- [9] Panchenko, M., A.I. Brazhenko, V.E. Shaposhnikov, A.A. Konovalenko, H.O. Rucker, Fine spectral structures in Jovian decametric radio emission observed by ground-based radio telescope, EPSC2014-519, Cascais, Portugal, 2014.
- [10] Zheleznyakov, V.V., E.Y. Zlotnik, Cyclotron wave instability in the corona and origin of solar radio emission with fine structure. III. Origin of zebra-pattern. Solar Phys. 44, 461–470, 1975.

## The Mars aurora: UV detections and in situ electron flux measurements

**J.-C. Gérard** (1), L. Soret (1), R. Lundin (2), L. Libert (1), A. Stiepen (1), A. Radioti (1), J.-L. Bertaux (3), V.I. Shematovich (4) and D.V. Bisikalo (4)

(1) LPAP, Université de Liège, Belgium, (2) Institutet för Rymdfysik (IRF), Umeå, Sweden, (3) LATMOS, Université de Versailles-St Quentin-en-Yvelines, France, (4) INASAN, Russian Academy of Sciences, Moscow, Russian Federation  
(jc.gerard@ulg.ac.be / Fax: +32-4-3669711)

### Abstract

A detailed search through the database of the SPICAM instrument on board Mars Express made it possible to identify 16 signatures of the CO Cameron and CO<sub>2</sub><sup>+</sup> doublet auroral emissions. These auroral UV signatures are all located in the southern hemisphere in the vicinity of the statistical boundary between open and closed field lines. The energy spectrum of the energetic electrons was simultaneously measured by ASPERA-3/ELS at higher altitude. The UV aurora is generally shifted from the region of enhanced downward electron energy flux by a few to several tens of degrees of latitude, suggesting that precipitation occurs in magnetic cusp like structures along inclined magnetic field lines. The ultraviolet brightness shows no proportionality with the electron flux measured at the spacecraft altitude. The Mars aurora appears as a sporadic short-lived feature. Results of Monte Carlo simulations will be compared with the observed brightness of the Cameron and CO<sub>2</sub><sup>+</sup> bands.

### 1. Introduction

The presence of an auroral emission in the Mars nightside atmosphere was first detected during a limb observation performed on 11 August 2004 with the Spectroscopy for Investigation of Characteristics of the Atmosphere of Mars (SPICAM) UV spectrograph on board Mars Express by Bertaux et al. (2005). The auroral spectra showed the CO Cameron bands and the CO<sub>2</sub><sup>+</sup> doublet at 288.3 and 289.6 nm.

Energetic electron spike events have previously been detected in regions of maximal crustal magnetic field radial component by Mitchell et al. (2001) who interpreted these measurements as evidence of past or present reconnection of the residual magnetic field lines to the interplanetary magnetic field lines. Peaked electron distributions have been measured

with MAG/ER on board the Mars Global Surveyor (MGS) satellite (Brain et al., 2006) and by the ASPERA-3 set of plasma instruments on Mars Express (Lundin et al., 2006a, 2006b). These peaked electron distributions are considered as signatures of acceleration by electric fields along magnetic field lines. Lundin et al.'s (2006b) observations suggested that open magnetic field regions analogous to Earth's polar cusps are present near strong and moderate crustal fields on the Martian nightside. Halekas et al. (2008) identified localized events detected in strong magnetic cusp regions and sometimes associated with signatures of field-aligned currents, similar in several aspects to terrestrial cusp aurora.

### 2. Observations

The duration of the auroral detection by SPICAM may be used to estimate the latitudinal width of the aurora. We assume that the aurora is located at an altitude  $Z_{\text{aur}} \sim 130$  km, in agreement with the limb observations by Bertaux et al. (2005a) and a recent study of three auroral detected made at the limb with SPICAM by Soret et al. (this session). The estimated latitudinal size of the region of precipitation is thus small, ranging from 21 km to 125 km, with most values less than 60 km. These widths are comparable to or less than those derived from localized electron flux measurements by MGS and ASPERA-3.

All UV auroral detections are located in the southern hemisphere between 17.3° and 64.1° S and in a restricted longitude sector extending from 158° to 214°, a region where the crustal magnetic field is relatively large. More specifically, the UV aurora is observed in boundary regions between closed and open field lines as shown in Figure 1. It shows the position of the UV aurora (white dots) and the ground track of the corresponding Mars Express orbits overlaid on a map of the probability to find a closed magnetic field line derived from the

magnetometer/electron reflectometer measurements on board MGS.

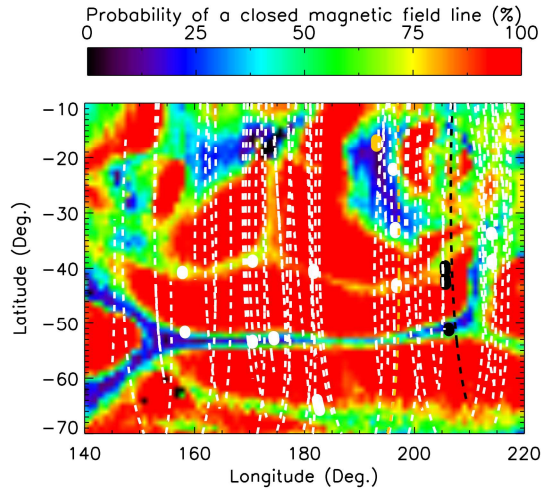


Figure 1: Ground tracks of Mars Express orbits (white dashed line) passing within 5 degrees of longitude of detections of UV aurora (white dots) overlaid on a map of the probability to find a closed magnetic field line at ~400 km. The light brown and the black circles indicate detections for which the SPICAM slit projection passed nearby within two days from the auroral events during other orbits (dashed lines, same colors as circles).

### 3. Discussion and Conclusions

Some of the characteristics of the auroral UV aurora and their relation to in situ electron precipitation measurements at higher altitude clearly appear:

- the Mars aurora is a spatially localized phenomenon located near the open-closed magnetic field line boundary in cusp-like structures
- the observed nadir brightness occasionally reaches as much as ~2.0 kR in the CO Cameron bands
- a majority of the passes over the “auroral” regions at different times and dates shows no evidence of UV auroral events. This suggests an infrequent phenomenon, but can also result from a combination of the SPICAM sensitivity, and the spatial-temporal variability of the phenomena.
- no clear correlation is observed with the down going electron energy flux measured at higher altitude with ASPERA-ELS
- the location of the footprint of the magnetic field line threading the peak in the electron flux may be shifted by several degrees from the sub-satellite

latitude, indicating that the local field lines are tilted from the vertical.

The lack of proportionality between the auroral brightness and the downward energy flux is somewhat measured by ASPERA is unexpected. If, as suggested by ASPERA measurements of upward moving ions, a quasi static potential totally or partly located below the spacecraft accelerates the electrons downward, the electron energy flux reaching the denser atmosphere can be drastically higher than the *in situ* measurement. In this case, the ultraviolet aurora will be more intense than expected from the energy flux measured at higher altitude. The geometry of nadir observations of field-aligned auroral emissions may also explain lower brightness than expected from a nadir observation.

The inclination angles derived from MGS MAG/ER measurements during localized events vary from  $83.2^\circ$  (B field pointing downward nearly vertically) to  $0.2^\circ$  (quasi horizontal). Translating the time delays between the SPICAM and the ASPERA auroral peaks in terms of orientation of the local B-field, the tilt angles from nadir vary from  $\sim 3^\circ$  (quasi vertical) to  $\sim 55^\circ$ . We also note that the lack of auroral persistency observed with SPICAM (see Figure 1) raises questions about the global versus local context of aurora at Mars. Aurora may be more frequent on a global scale, like the terrestrial aurora, but less frequent on a local scale, in view of the difference between a global dipole magnetic field and the complexity of the Martian crustal magnetic field. All together, it appears that the UV aurora is most likely associated with the localized and/or temporarily variable phenomena.

A likely scenario is that the aurora is produced by electron acceleration in parallel electric fields associated with upward field aligned currents generating peaked electron distributions. They can arise on the boundary between closed and open residual field lines as a consequence of the shears of the flow velocity of the magnetosheath or magnetospheric plasmas.

### Acknowledgements

We gratefully thank all members of the ESA Mars Express project and of the SPICAM and ASPERA-3 scientific and technical teams. This research was supported by the PRODEX program managed by the European Space Agency with the help of the Belgian Federal Space science Policy Office. This work was also funded by the Centre National d’Etudes Spatiales.

## References

- Bertaux, J.-L., F. Leblanc, O. Witasse, E. Quemerais, J. Lilensten, S. A. Stern, B. Sandel and O.Korablev, Discovery of an aurora on Mars, *Nature*, 435, 790-794, 2005.
- Brain, D. A., J. S. Halekas, L. M. Peticolas, R. P. Lin, J. G. Luhmann, D. L. Mitchell, G. T. Delory, S.W. Bougher, M. H. Acuña, and H. Rème, On the origin of aurorae on Mars, *Geophys. Res. Lett.*, 33, L01201, 2006.
- Halekas, J. S., D. A. Brain, R. P. Lin, J. G. Luhmann, and D. L. Mitchell, Distribution and variability of accelerated electrons at Mars, *Adv. Space Res.*, 41, 1347–1352, 2008.
- Lundin, R., et al., Plasma acceleration above Martian magnetic anomalies, *Science*, 311, 980-983, 2006a.
- Lundin, R., et al., Ionospheric plasma acceleration at Mars: ASPERA-3 results, *Icarus*, 182, 308-319, 2006b.
- Mitchell, D. L., R. P. Lin, C. Mazelle, H. Rème, P. A. Cloutier, J. E. P. Connerney, M. H. Acuña, and N. F. Ness (2001), Probing Mars' crustal magnetic field and ionosphere with the MGS Electron Reflectometer, *J. Geophys. Res.*, 106, 2001.
- Soret, L. et al., Limb observations and modeling of Mars aurorae, submitted.



## Altitude of Mars aurorae deduced from SPICAM limb detections

**L. Soret** (1), J.-C. Gérard (1), L. Libert (1), V. I. Shematovich (2), D. V. Bisikalo (2), A. Stiepen (1) and J.-L. Bertaux (3)  
(1) Laboratoire de Physique Atmosphérique et Planétaire, Université de Liège, Liège, Belgium  
(2) Institute of Astronomy, Russian Academy of Sciences, Moscow, Russia  
(3) LATMOS, Université de Versailles Saint-Quentin-en-Yvelines, Guyancourt, France  
(Lauriane.Soret@ulg.ac.be / Fax: +32-43669729)

### Abstract

Martian aurorae have been detected with the SPICAM instrument on board Mars Express both in the nadir and the limb viewing modes. In this study, we focus on three limb detections to determine the altitudes of the auroral emissions and their intensities. We then use a model of electron transport in the Martian thermosphere based on a Monte-Carlo method to simulate and to understand the excitation processes leading to these auroral emissions.

### 1. Introduction

The first Martian aurora was detected by [1] with SPICAM, in a limb observation. [2] discovered several other aurorae in nadir observations and one additional limb detection. Nadir observations were studied in more details by [3]. Here, we added a third limb detection to this list, based on a search of the entire SPICAM limb observations database.

The UV aurorae observed in the Martian atmosphere include the CO ( $a^3\Pi - X^1\Sigma$ ) Cameron bands between 180 and 240 nm, the CO ( $A^1\Pi - X^1\Sigma^+$ ) Positive system (CO 4P) between 135 and 170 nm, the  $\text{CO}_2^+$  ( $B^2\Sigma_u^+ - X^2\Pi_g$ ) doublet near 289 nm, the OI multiplet at 297.2 nm and the 130.4 nm OI emission.

### 2. Data analysis

The altitude of the CO Cameron bands emission was found to be  $137 \pm 27$  km. The intensities of the auroral emissions have also been quantified. The mean intensities deduced for these emissions reach 2500 R, 500 R, 650 R, 360 R and 30 R for the CO Cameron bands, the CO Positive system, the  $\text{CO}_2^+$ , the OI multiplet at 297.2 nm and the 130.4 nm OI emission, respectively. As already noticed by [2] and [3], Mars

aurorae occur at the statistical boundary of open-closed magnetic field lines, in cusp-like structures.

### 3. Modelling

The Monte-Carlo model of electron transport in the Martian thermosphere implemented by [4] and [5] can reproduce auroral emissions either using mono-energetic electron distributions or ASPERA-3/ELS electron energy spectra as input parameters. Results obtained with mono-energetic distributions ranging from 50 to 1000 eV simulate auroral emissions occurring between 117 and 141 km, in agreement with the observations. The model also well reproduces the observed altitudes of the aurorae with electron energy spectra measured with the ASPERA-3/ELS instrument.

### 4. Summary and Conclusions

Limb observations of Martian aurorae are useful to determine the intensities of the auroral emissions and their altitudes. The Monte-Carlo model of electron transport in the Martian thermosphere correctly reproduces the altitude of the aurorae but the predicted vertically integrated intensities appear to be overestimated, probably as a consequence of the inclination and curvature of the magnetic field line threading the aurora. The intensity ratio of the CO and  $\text{CO}_2^+$  emissions is in good agreement with the limb observations though.



## Acknowledgements

We gratefully thank all members of the ESA Mars Express project and of the SPICAM and ASPERA-3 scientific and technical teams. We also thank S. Bougher for providing the neutral atmosphere modeled by its M-GITM and R. Lundin for the ASPERA-3/ELS electron energy spectra used for the Monte-Carlo simulations. This research was supported by the PRODEX program managed by the European Space Agency with the help of the Belgian Federal Space science Policy Office. This work was also funded by the Centre National d'Etudes Spatiales.

## References

- [1] Bertaux, J.-L., Leblanc, F., Witasse, O., Quemerais, E., Lilensten, J., Stern, S. A., Sandel, B. and Korabev, O. (2005), Discovery of an aurora on Mars, *Nature*, 435, 790-794, doi:10.1038/nature03603.
- [2] Leblanc, F., et al. (2008), Observations of aurorae by SPICAM ultraviolet spectrograph on board Mars Express: Simultaneous ASPERA-3 and MARSIS measurements, *J. Geophys. Res.*, 113, A08311, doi: 10.1029/2008JA013033.
- [3] Gérard, J.-C., Soret, L., Libert, L., Lundin, R., Stiepen, A., Radioti, A. and Bertaux, J.-L., Concurrent observations of ultraviolet aurora and energetic electron precipitation with Mars Express, submitted.
- [4] Shematovich, V. I., Bisikalo, D. V. and Gérard, J.-C. (1994), A kinetic model of the formation of the hot oxygen geocorona: 1. Quiet geomagnetic conditions. *Journal of Geophysical Research: Space Physics*, 99(A12), 23217-23228, doi :10.1029/94JA01769.
- [5] Shematovich, V. I., Bisikalo, D. V., Gérard, J.-C., Cox, C., Bougher, S. W. and Leblanc, F. (2008). Monte Carlo model of electron transport for the calculation of Mars dayglow emissions. *Journal of Geophysical Research: Planets*, 113(E2), doi: 10.1029/2007JE002938.

## Variable opening angle of emission cone of Jovian decameter radiation generated by cyclotron maser instability

**P. H. M. Galopeau** (1), M. Y. Boudjada (2), and H. O. Rucker (3)

(1) LATMOS-CNRS, Université Versailles Saint-Quentin-en-Yvelines, Guyancourt, France, (2) Space Research Institute, Austrian Academy of Sciences, Graz, Austria, (3) Astronomy Commission, Austrian Academy of Sciences, Graz, Austria (patrick.galopeau@latmos.ipsl.fr)

### Abstract

A recent study of the Io-controlled Jovian decameter radiation revealed that the radio emission is beamed in a hollow cone which presents a flattening in a specific direction linked to the local magnetic field in the source. We investigate some reasons for the existence of such a flattening. The Jovian decameter radiation, like the other auroral radio emissions emanating from the magnetized planets in the solar system, is known to be produced by the cyclotron maser instability (CMI). This mechanism allows the direct amplification of the waves through a resonant coupling between the electron population of the plasma and the electromagnetic

waves with right circular polarization of the X mode. In a medium with axial symmetry, i.e., where  $\mathbf{B}$  and  $\nabla B$  are parallel, this amplification is maximum for a particular value of the emergence angle relatively to the local magnetic field  $\mathbf{B}$ . We suppose that the plasma is constituted of a cold component which supports the wave propagation and an energetic component which takes part in the growth of the waves by supplying the CMI with free energy. When  $\mathbf{B}$  and  $\nabla B$  are not parallel, the angle corresponding to the maximum amplification is not constant anymore, so that the emission cone does not have any axial symmetry and then presents a flattening; it is the case of the Io-controlled Jovian decameter radiation.

# Background Non-Uniform Wind Effect on Large Scale Zonal Flow Generation by ULF Modes

**Kh. Chargazia** (1,2), O. Kharshiladze (2)

(1) I. Vekua Institute of Applied Mathematics of Tbilisi State University, Tbilisi, Georgia,

(2) M. Nodia Institute of Geophysics of Tbilisi State University, Tbilisi, Georgia (khatuna.chargazia@gmail.com)

## Abstract

In the present work the features of generation of the large scale flows in the ionosphere on the background of inhomogeneous non-stationary winds is considered. From the equation of magnetized (modified by the geomagnetic field) Rossby type waves using multi-scale expansion the nonlinear equation of interaction of amplitudes of five different scale modes is obtained. These modes are: ultra low frequency (ULF) primary magnetized Rossby wave, its two satellites, long wavelength zonal mode and large scale background mode (inhomogeneous wind). The effects of nonlinearities (scalar, vector) in formation of the large scale zonal flows by magnetized Rossby waves with finite amplitudes in the dissipative ionosphere is studied. For this purpose the modified parametric approach is used. New mechanism of energy exchange between the small scale waves and large scale ones are revealed.

## 1. Introduction

Recently interest to generation of the large scale zonal flows, influencing the transfer processes in the atmosphere [9], magnetized plasma [10], in some astrophysical objects [11] has increased. Excitation of the anisotropic large-scale structures, such as the zonal flows, streamers and convective cells by comparably small scale turbulence is intensively studied in laboratory plasma [10], as well as in geophysical and astrophysical flows [11].

The different scale wave perturbations undergo amplification/generation at the presence of the background shear flow and the nonlinear effects appear important in their dynamics [19]. Nonlinear interaction of the waves with each other and medium can generate various nonlinear structures - comparably large scale zonal flows among them [17]. Theory of generation of the zonal flows by Rossby waves were developed in works [14,24] using the

parametric formalism on the basis of three wave nonlinear interaction.

## 2. Model Equation for magnetized Rossby wave

For investigation of the interaction of the Rossby type waves with local inhomogeneous zonal wind the nonlinear equation of the dynamics of magnetized Rossby type structures in the ionosphere is used:

$$\left( \frac{\partial}{\partial \tau} + V_0(y) \frac{\partial}{\partial x} \right) (P - \Delta P) + (V_R + V_0^*) \frac{\partial P}{\partial x} - b_{\perp 0} \frac{\partial^2 P}{\partial y^2} - b_{\perp z} \frac{\partial^2 P}{\partial x^2} + \nu \Delta^2 P = -V_R P \frac{\partial P}{\partial x} + J(P, \Delta P). \quad (1)$$

Here the following dimensionless variables are used:

$$\begin{aligned} \tau &= 2\Omega_{0z} t; \quad P = P / P_0; \quad x, y = (x, y) / r_R; \quad \alpha + \beta = \partial \bar{\Omega} / \partial y, \\ \alpha + \beta &= (\alpha + \beta) r_R / \bar{\Omega}; \quad V_0^* = d^2 V_0 / dy^2; \quad V_0 = V_0 / (2\Omega_{0z} r_R); \\ b_{\perp z} &= b_{\perp z} / (2\Omega_{0z}); \quad b_{\perp z} = \sigma_{\perp} B_{0z}^2 / (\rho_0 c^2); \quad \nu = \nu / (2\Omega_{0z} r_R^2); \\ J(a, b) &= \partial a / \partial x \cdot \partial b / \partial y - \partial a / \partial y \cdot \partial b / \partial x; \quad b_{\perp 0} = \sigma_{\perp} B_0^2 / (\rho_0 c^2); \\ b_{\perp 0} &= b_{\perp 0} / (2\Omega_{0z}). \end{aligned}$$

Equation (1) represents the generalized Charney-Obukhov-Hasegawa-Mima equation.

## 3. Multiscale representation of perturbed quantities

In the paper a five wave process is investigated – nonlinear interaction of comparably small scale initial pumping waves (magnetized Rossby waves), its two satellites, large scale zonal modes and more larger shear flows. Using standard decomposition formalism (multiscale expansion) for perturbed values we will have the following representation:

$$\begin{aligned}\hat{P}(x, y, t) &= \hat{P}_0(y, k) e^{i(q_x x - \Omega t)} + \hat{P}_0^*(y, k) e^{-i(q_x x - \Omega t)}, \\ \tilde{P}_0(x, t) &= \tilde{P}_0 e^{i(k_x x - \omega_k t)} + \tilde{P}_0^* e^{-i(k_x x - \omega_k t)}, \\ \tilde{P}_\pm(x, y, t) &= \tilde{P}_\pm(y, k) e^{i(k_\pm x - \omega_\pm t)} + \tilde{P}_\pm^*(y, k) e^{-i(k_\pm x - \omega_\pm t)}.\end{aligned}$$

Here  $k_\pm = k_x \pm q_x$ ,  $\omega_\pm = \omega_k \pm \Omega$ ; sign “\*” denotes complex conjugate; the pairs  $(\omega, k_x \cdot \mathbf{e}_x)$  and  $(\Omega, q_x \cdot \mathbf{e}_x)$  – are frequencies and wave vectors of comparably small scale pumping wave and the large scale zonal flow, respectively.

## 4. Summary and Conclusions

In the presented paper nonlinear generation and further evolution of large scale zonal flows according to the small scale ULF magnetized Rossby waves with finite amplitude in a shear flow driven dissipative ionosphere is studied. Initial nonlinear dynamic Charney – Obukhov equations, containing a scalar as well as vector nonlinearity and describing the features of turbulent behavior of magnetized Rossby waves are obtained. Parametric approach and five wave presentation of the perturbations is used. On the basis of the dynamic equation the system of three connected equations for amplitudes of satellite waves and generated zonal modes at given profiles of pumping waves and background shear flow are obtained. On the basis of theoretical analysis of the corresponding system of equations for amplitudes of perturbations new features of energy pumping from comparably small scale ULF magnetized Rossby waves and shear flows into the large scale zonal flows and of nonlinear self organization of collective activity of the five waves in the ionospheric medium.

From analysis it follows that comparably small scale magnetized Rossby waves appear modulationally unstable with respect to the large scale flows. This instability is accompanied with excitation of the large scale zonal flows.

This investigation has revealed a possible mechanism of generation, intensification (weakening) of the zonal flows by finite amplitude Rossby waves in the ionosphere by virtue of the local background flows depending on the parameters of this flow. Herewith, the background flow with approximately small amplitude stipulates development of modulation instability and intensification of the zonal flow generation, increasing growth increment. But strong shear flow

sufficiently decrease instability increment and accordingly the process of zonal flow generation weakens.

Reinolds stress acts as initial mechanism for instability swinging. Spectral energy pumping from small scale Rossby wave and background shear flow into large scale zonal flow in the ionospheric medium. Thus magnetized Rossby wave type fluctuation can destabilized due to nonlinear five-wave interaction with simultaneous generation of the large scale zonal flows.

## Acknowledgements

The work is done by support of grant No 31/14 of Shota Rustaveli National Science Foundation.

## References

- [1] Galperin, B, Sukoriansky, S., Dikovskaya N., et al.: Nonlinear Process. Geophys, 13, 83, 2006.
- [2] Diamond, P., Itoh, S., Itoh, K. and Hahm T.S.: Plasma Phys. Control. Fusion, 47, R35, 2005.
- [3] Fridman, A.: Prospects of Phys. Sciences, 177, 2, 121, 2007.
- [4] Shukla, P. and Stenflo, L.: Phys. Lett. A, 307, 154, 2003.
- [5] Rhines, P.: Chaos, 4, 313, 1994.
- [6] Petviashvili, V and Pokhotelov, O.: Solitary waves in plasma and atmosphere, M. Energoatomizdat, 1989 (in Russian)
- [7] Onishchenko, O., Pokhotelov, O., Sagdeev, R. et al.: Nonlin. Proc. Geophys., 11, 241, 2004.

# Discovery of Diffuse Aurora on Mars

A. Stiepen<sup>1,2</sup>, N.M. Schneider<sup>1</sup>, S.K. Jain<sup>1</sup>, J. Deighan<sup>1</sup>, A.I.F. Stewart<sup>1</sup>, J.S. Evans<sup>3</sup>, M.H. Stevens<sup>4</sup>, D. Larson<sup>5</sup>, D. Mitchell<sup>5</sup>, F. Montmessin<sup>6</sup>, M.H. Chaffin<sup>1</sup>, W.E. McClintock<sup>1</sup>, J.T. Clarke<sup>7</sup>, G.M. Holsclaw<sup>1</sup>, and B.M. Jakosky<sup>1</sup>

(1) Laboratory for Atmospheric and Space Physics, University of Colorado, (2) Laboratoire de Physique Atmosphérique et Planétaire (LPAP), University of Liège, Belgium ([arnaud.stiepen@ulg.ac.be](mailto:arnaud.stiepen@ulg.ac.be)), (3) Computational Physics, Inc, (4) Space Science Division, Naval Research Laboratory, (5) Space Sciences Lab, U. California, Berkeley, (6) LATMOS/IPSL, Guyancourt, France, (7) Center for Space Physics, Boston University ([arnaud.stiepen@ulg.ac.be](mailto:arnaud.stiepen@ulg.ac.be))

## Abstract

The Imaging Ultraviolet Spectrograph (IUVS, McClintock et al., 2014) onboard the MAVEN spacecraft has discovered diffuse aurora in Mars' northern hemisphere spanning a wide range of geographic latitudes and longitudes (Figure 1). This widespread aurora differs from the small auroral patches discovered by the SPICAM instrument onboard the Mars Express spacecraft (Bertaux et al., 2005; Leblanc et al., 2008; Gérard et al., submitted; Soret et al., submitted) restricted to regions of crustal magnetic fields in the southern hemisphere. Furthermore, the northern diffuse aurora appears to peak at altitudes below 100 km, while the crustal field aurora peaked around 120 km.

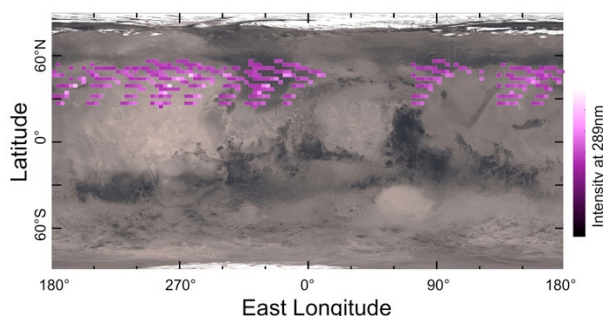


Figure 1: Mapping of the detection of the aurora.

## 1. Discovery of a new type of Martian aurora

An increase of the intensity of the  $\text{CO}_2^+$  289 nm nightside emission was observed by IUVS from Dec, 18th to Dec, 23rd, 2014. During the same period, the Solar Energetic Particle (SEP) instrument and the Solar Wind Electron Analyzer (SWEA) instrument on board MAVEN measured important high-energy electron fluxes. We suggest that high-energy electrons carried by the Interplanetary Magnetic Field (IMF) deposit their energy in the Mars' atmosphere to produce ultraviolet diffuse aurora.

## 2. Source of the aurora

The source of the energetic particles appears to be the Sun, based both on the depth of atmospheric penetration and the timing of a substantial increase in energetic electrons during the aurora. Electrons with ~20 keV measured by the SEP instrument over the same period than the detection of the ultraviolet aurora by IUVS are capable to travel along open field lines and penetrate in the Mars' atmosphere below 100 km. A second event of lesser magnitude was observed in both auroral emission and solar energetic particles on 3 March 2015, confirming the correlation.

## 3. Spectral analysis

The observed auroral spectrum resembles Mars dayglow (see Figure 2; e.g Leblanc et al., 2006; Stiepen et al., 2015), though the relative strength of spectral features differs due to the different excitation caused by 20 keV electrons in comparison with solar EUV radiation.

We carefully verified the presence of the  $\text{CO}_2^+$  doublet at 289 nm and the CO Cameron bands on every spectrum taken by IUVS during the period the aurora was observed. During that period, the aurora could be spectrally identified in all IUVS nightside periapse observations.

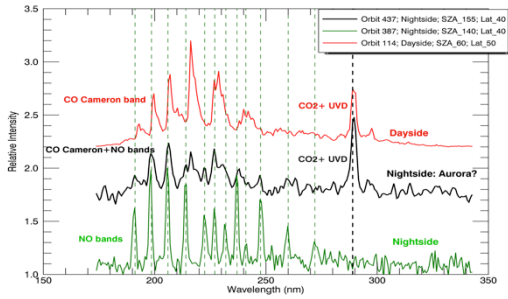


Figure 2: Comparison of IUVS dayglow (red), nightglow (green) and nightglow and auroral (black) spectrum

## 4. Summary and Conclusions

We report the discovery of diffuse ultraviolet aurora in Mars' Northern Hemisphere. We suggest that these auroras are produced by precipitation of high energetic electrons carried by the IMF.

MAVEN's complement of remote sensing and in situ instruments may offer the best opportunity to study diffuse auroral processes associated with open field lines, as may occur on unmagnetized or weakly magnetized bodies in the Solar System.

Future work will consist in quantitative comparison of the aurora brightness and altitude with electron precipitation models and further comparison to crustal field aurora.

## Acknowledgements

A. Stiepen was supported by the Belgian American Educational Foundation, the Rotary District 1630 and Prodex program of BELSPO.

## References

Bertaux, J.-L. et al., 2005, 2006. Gérard et al., submitted. Leblanc et al., 2006, 2008. McClintock, W. E. et al., 2014. Soret et al., submitted. Stiepen, A. et al., 2015.



## Europa's neutral and plasma environment investigated through FUV aurora imaging

**L. Roth** (1,2), K. D. Retherford (2), J. Saur (3), D. F. Strobel (4), P. D. Feldman (4), M. A. McGrath (5), F. Nimmo (6), J. R. Spencer (7), C. Grava (2), and A. Blöcker (3)

(1) Space and Plasma Physics, Royal Institute of Technology KTH, Stockholm, Sweden (lorenzr@kth.se)

(2) Southwest Research Institute, San Antonio, TX, USA

(3) University of Cologne, Germany

(4) Johns Hopkins University, Baltimore, MD, USA

(5) SETI Institute, Mountain View, CA, USA

(6) University of California Santa Cruz, CA, USA

(7) Southwest Research Institute, Boulder, CO, USA

### Abstract

Within two recent Hubble Space Telescope (HST) campaigns, Europa's FUV aurora was imaged by Hubble's Space Telescope Imaging Spectrograph (STIS) on 16 days between January 2014 and April 2015. On each day several images of the hydrogen and oxygen emissions were obtained to follow up on the STIS detection of water vapor aurora in December 2012 [1]. We investigate the emission brightness, morphology and time-variability in all images to systematically characterize Europa's FUV aurora. Thereby, we search for influences of the magnetospheric environment on the emission and for potential atmospheric asymmetries like localized water vapor plumes.

### 1. Introduction

With its subsurface water ocean [2] and relatively young icy surface [3] Europa is generally considered a prime candidate in the search for present-day habitable environments in our solar system. Spectral UV images taken by STIS taken in 2012 revealed first signs of active water vapor plumes at Europa's south pole. The UV images are, however, not only a tool to study the atmosphere and plumes, but also to investigate the plasma environment that significantly affects the electron-excited aurora.

### 2. Technique

The observations of atomic FUV emissions near Europa provide an excellent opportunity to investigate both the neutral and plasma environment

[4,5]. Neutral hydrogen and oxygen in Europa's environment can be observed through electron-excited emissions and solar fluorescence at HI 1216 Å (Lyman- $\alpha$ ), OI 1304 Å and OI 1356 Å. In Europa's sputtering-generated global atmosphere that consists mainly of molecular oxygen O<sub>2</sub>, electron excited OI 1356 Å emissions are brighter than the OI 1304 Å aurora. Because electron impact on H<sub>2</sub>O yields Lyman- $\alpha$  and OI 1304 Å but relatively little OI 1356 Å [6], enhanced emission at Lyman- $\alpha$  and OI 1304 Å are diagnostic for H<sub>2</sub>O abundance.

### 3. Observations

Spatial-spectral observations of Europa were taken by STIS on 16 occasions simultaneously imaging the moon at the HI 1216 Å (Lyman- $\alpha$ ), OI 1304 Å and OI 1356 Å lines. First follow-up HST observations after the plume detection [1] from January and February 2014 were timed to observe Europa near orbital apocenter to test the hypothesis that the plume activity is correlated with the orbital position. No local H and O emissions were detected in these images [7]. Between November 2014 and April 2015 Europa was observed again during 14 visits by Hubble. On four of these occasions Europa was imaged in eclipse, allowing to measure H and O auroral brightnesses in the absence of sunlight.

### 4. Analysis

We systematically analyze the total brightness of the oxygen emissions and the spatial morphology across the disk. In order to determine the influence of the highly variable plasma environment, which co-rotates with Jupiter's ~10 hour period, we study the

time-variability within the several hour long observing visits. The relative brightness of the two oxygen lines at 1356 Å and 1304 Å will allow to constrain relative abundances of molecular and atomic oxygen. Furthermore, we determine the atmospheric H Lyman- $\alpha$  brightnesses and thereby constrain local H<sub>2</sub>O plume abundances in all images.

## Acknowledgements

L. R. acknowledges support from the Swedish Governmental Agency for Innovation Systems “VINNOVA”, which is partly funded by the EU Marie Curie programme. The work in this study has been partially inspired by the activities of the ISSI International Team #322.

## References

- [1] Roth, L., et al. "Transient water vapor at Europa's south pole." *Science* 343.6167 (2014): 171-174.
- [2] Khurana, K. K., et al. "Induced magnetic fields as evidence for subsurface oceans in Europa and Callisto." *Nature* 395.6704 (1998): 777-780.
- [3] Greeley, Ronald, et al. "Geology of Europa." *Jupiter: The Planet, Satellites and Magnetosphere* (2004): 329-362.
- [4] McGrath, M. A., C. J. Hansen, and A. R. Hendrix. "Observations of Europa's tenuous atmosphere." Chapter in *Europa*. University of Arizona Press, Tucson 85 (2009).
- [5] Saur, J., et al. "Hubble space telescope/advanced camera for surveys observations of Europa's atmospheric ultraviolet emission at eastern elongation." *The Astrophysical Journal* 738.2 (2011): 153.
- [6] Makarov, Oleg P., et al. "Kinetic energy distributions and line profile measurements of dissociation products of water upon electron impact." *J. of Geophysical Res.: Space Physics* (1978–2012) 109.A9 (2004).
- [7] Roth, L., et al. "Orbital apocenter is not a sufficient condition for HST/STIS detection of Europa's water vapor aurora." *Proceedings of the National Academy of Sciences* 111.48 (2014): E5123-E5132.

# Auroral Electron Energy Estimation Using H/H<sub>2</sub> Brightness Ratio Applied to Jupiter Aurora

C. Tao (1), L. Lamy (2), R. Prangé (2), N. André (1), and S. V. Badman (3)

(1) IRAP, Université de Toulouse/UPS-OMP/CNRS, Toulouse, France, (2) LESIA, Observatoire de Paris-CNRS, France, (3) Lancaster University, Lancaster, UK. (chihiro.tao@irap.omp.eu)

## Abstract

The measurement of the H/H<sub>2</sub> brightness ratio of giant planets' far-ultraviolet (FUV) aurora is a proxy for the characteristics of precipitating electrons. Here, we check the relevance of this H/H<sub>2</sub> indicator with the Jupiter auroral observations obtained by the Hubble Space Telescope (HST) and compare it with (i) results evaluated from another technique at Jupiter (the FUV color ratio (CR) method) and (ii) results obtained with the same technique at Saturn.

An analysis of Saturn's southern aurorae with the Ultraviolet Imaging Spectrograph (UVIS) instrument onboard the Cassini spacecraft showed that the brightness ratio of H Lyman- $\alpha$  to H<sub>2</sub> auroral emissions statistically decreases with the brightness of H<sub>2</sub> taken as a proxy of the energy of precipitating electrons [1]. This measurement was then investigated in details in the Saturn's case by [2] to show that the brightness ratio provides a sensitive diagnosis of low energy electrons (typically lower than 10 keV), in contrast with the FUV CR method which provides the energy of electrons > 10 keV [3]. Energy-flux relation converted from the observation using models shows different trend in the lower energy range (< a few keV) compared to the higher energy range (> a few keV), reflecting different magnetosphere-ionosphere processes [2]. Therefore, the H/H<sub>2</sub> index would be also useful for the Jupiter case to investigate the role of low energy auroral electrons.

Since HST observes Jupiter from the orbit around the Earth, it contains Lyman- $\alpha$  emissions from geocoronal hydrogen atoms. Jupiter's coronal emission also contributes. We remove these contaminations by subtracting the emission at the disc. The H/H<sub>2</sub> ratio is then evaluated by spectral fitting as in [1]. We use HST/STIS long-slit spectra taken on the first half of January 2014 (ID: GO13035).

As a result, we show that the H/H<sub>2</sub> brightness ratio decreases with increasing H<sub>2</sub> brightness, which is qualitatively similar to the Saturn's case, but with different quantitative values. The H/H<sub>2</sub> ratio still decreases at large H<sub>2</sub> intensity case, which indicates the existence of H at the low altitude. On the other hand, larger sensitivity on the H/H<sub>2</sub> for the main auroral emission at the limb compared to the CR method indicates a better sensitivity of the H/H<sub>2</sub> ratio at lower electron energy.

## Acknowledgements

This work uses observations made with the NASA/ESA Hubble Space Telescope (observation ID: GO13035), obtained at the Space Telescope Science Institute, which is operated by AURA, Inc. for NASA. This research was supported by a grant-in-aid for Scientific Research from the Japan Society for the Promotion of Science (JSPS).

## References

- [1] Lamy, L., R. Prangé, W. Pryor, J. Gustin, S. V. Badman, H. Melin, T. Stallard, D. G. Mitchell, and P. C. Brandt: Multispectral simultaneous diagnosis of Saturn's aurorae throughout a planetary rotation, *J. Geophys. Res. Space Physics*, 118, 4817–4843, doi:10.1002/jgra.50404, 2013.
- [2] Tao, C., L. Lamy, and R. Prangé: The brightness ratio of H Lyman- $\alpha$ /H<sub>2</sub> bands in FUV auroral emissions: A diagnosis for the energy of precipitating electrons and associated magnetospheric acceleration processes applied to Saturn, *Geophys. Res. Lett.*, 41, doi:10.1002/2014GL061329, 2014.
- [3] Gustin, J., J.-C. Gérard, W. Pryor, P. D. Feldman, D. Grodent, G. Holsclaw, Characteristics of Saturn's polar atmosphere and auroral electrons derived from HST/STIS, FUSE and Cassini/UVIS spectra, *Icarus*, 200, 176-187, 2009.



# Current-Voltage Relation View of Temporal/Spatial Variations of Jupiter Aurora: Hisaki and HST Comparison

C. Tao (1), T. Kimura (2), S. V. Badman (3), G. Murakami (4), K. Yoshioka (5), F. Tsuchiya (6), N. André (1), I. Yoshikawa (7), A. Yamazaki (4), D. Shiota (8), H. Tadokoro (9), and M. Fujimoto (4)

(1) IRAP, Université de Toulouse/UPS-OMP/CNRS, Toulouse, France, (2) Riken, Saitama, Japan, (3) Lancaster University, Lancaster, UK, (4) ISAS/JAXA, Sagamihara, Japan, (5) Rikkyo University, Tokyo, Japan, (6) Tohoku University, Sendai, Japan, (7) University of Tokyo, Tokyo, Japan, (8) Nagoya University, Nagoya, Japan, (9) Musashino University, Tokyo, Japan. (chihiro.tao@irap.omp.eu)

## Abstract

We investigate the temporal and spatial variations of the Jupiter aurora applying the power and color ratio (CR) relations using both Hisaki and Hubble Space Telescope (HST) data. Spatially-resolved HST observation shows the relation is different among auroral regions. Spatially-integrated continuous observation by Hisaki indicates the occurrence rate of polar-like events, i.e., large CR and small power based on HST results, becomes large during low solar wind dynamic pressure. For the auroral power enhancement events, two scenarios are proposed in the view point of source plasma variations derived from the relation.

## 1. Introduction

Ultraviolet (UV) emissions are from atmospheric H<sub>2</sub> and H excited by precipitating auroral electrons. The far-UV (FUV) color ratio (CR), defined as the ratio of the intensity of a waveband unabsorbed by hydrocarbons to that of an absorbed one, is usually used to estimate the auroral electron energy. The previous study shows high latitude emissions additionally show cases of high electron energies (large CR) with low energy flux [1]. The spectrometer EXCEED [e.g., 2] onboard JAXA's Earth-orbiting planetary telescope Hisaki monitors extreme UV emissions from Jovian aurora and Io plasma torus continuously. Hisaki succeeded to detect sporadic, large auroral power enhancements lasting both short (<1 planetary rotation) and longer variations [3]. The latter is mostly accompanied with solar wind dynamic pressure enhancements. In this study, we investigate (1) the time variation of power-CR relation in these events and (2) statistical survey for occurrence of polar-dominant events, using Hisaki and HST data.

## 2. Datasets and Analysis

The HST observations (ID: GO13035) acquired FUV images and spectra of Jupiter's northern aurora using the FUV-MAMA detector of STIS. The long slit G140L grating provides imaging spectra over 1100–1700 Å with ~12 Å resolution (Fig. 1). The typical CR for STIS spectra is defined as  $CR_{STIS} = I_{1550-1620 \text{ Å}} / I_{1230-1300 \text{ Å}}$ , where  $I$  is the height-integrated intensity of the emission in units of kR or photons/sec. Power of  $I_{1550-1620 \text{ Å}}$  is referred to as the auroral electron energy flux. 200 sec spectral observation is taken 14 times over the first 2 weeks on January 2014.

EXCEED counts photons over 800–1480 Å wavelength range with 3 Å resolution, over northern hemisphere (Fig. 1a).  $CR_{EXCEED}$  is newly defined as  $CR_{EXCEED} = I_{1385-1448 \text{ Å}} / I_{1263-1300 \text{ Å}}$ . The power representing energy flux is replaced by  $I_{1385-1448 \text{ Å}}$ . We used observation from 20 Dec. 2013 to Jan. 2014.

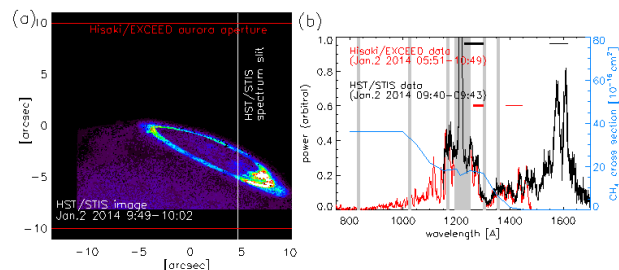


Figure 1. (a) HST auroral image and (b) auroral spectra taken by HST (black) and Hisaki (red).

## 3. Results

### 3.1 Power-CR Relation and Variation

The power- $CR_{STIS}$  relation is derived from HST/STIS spectra separating regions, i.e., main aurora and polar region, referring to the images taken in the same HST orbit (Fig. 2a). As the previous study [1], CR

increases with the power generally and the polar emission additionally contains low power and high CR components.

The power-CR<sub>EXCEED</sub> relation for EXCEED (Fig. 2b) shows similar scatters, with large power and medium CR for intensity enhanced events [3] both short- (orange, <1 rotation) and long- (light blue) durations.

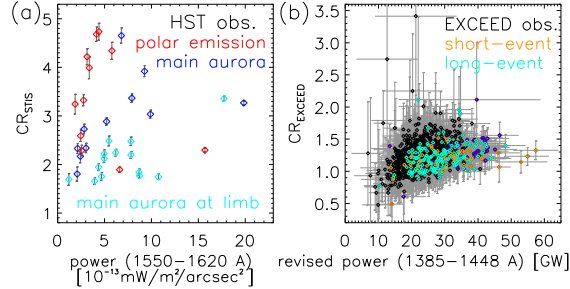


Figure 2. Power-CR relations derived using (a) HST and (b) Hisaki data, where the latter power is normalized by aperture.

### 3.2 Statistics of Polar-dominant Event

We select events with low power and large CR (Fig. 3a), which we take to represent events dominated by high latitude emission. These events are observed often at end of 2013 and Jan. ~10 (Fig. 3b). Solar wind pressure (blue line) and interplanetary magnetic field (IMF) sector (horizontal line for toward time) are estimated from the solar wind models [4, 5]. Occurrence of the polar-dominant events (orange & red) increases for low solar wind pressure period.

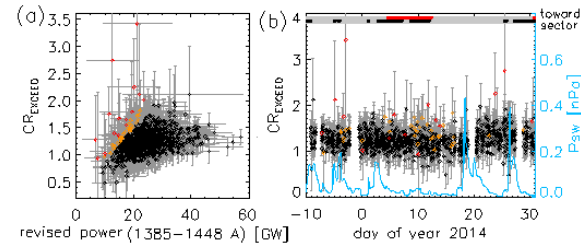


Figure 3. (a) Power-CR<sub>EXCEED</sub> relation and (b) time variations of CR<sub>EXCEED</sub>, solar wind dynamic pressure (blue line), and the IMF sector (horizontal bar).

## 4. Discussion

Time variation of the power-CR relation during auroral intensity enhancement events indicates source current density enhancements according to the Knight's auroral electron acceleration theory. Possible scenarios to explain the derived variations are (i) an adiabatic variation of the magnetospheric

plasma under a magnetospheric compression and/or plasma injection, and (ii) a change of the dominant power of auroral components from the main aurora to the emission at the open-closed boundary.

Potential causes for these observed potential-dominant events are (i) enhancements of the polar emission, (ii) relative increases of the polar emission in the total emission by a decrease in the main auroral oval emission, and/or (iii) rising of the hydrocarbons in the atmosphere to increase the absorption effect and CR.

## 5. Conclusions

We derive power-CR relations using spatially-resolved HST data and continuous observation enabled by Hisaki. Characteristic power-CR relation of polar region, i.e., small power and large CR, is often observed during small solar wind dynamics pressure periods. The auroral intensity enhancements associated with flux enhancements, rather than the energy, indicates source current enhancements.

## Acknowledgements

We acknowledge working teams of Hisaki/EXCEED. This work uses observations made with the NASA/ESA HST (observation ID: GO13035), obtained at the Space Telescope Science Institute, which is operated by AURA, Inc. for NASA. This research was supported by a grant-in-aid for Scientific Research from the Japan Society for the Promotion of Science (JSPS).

## References

- [1] Gustin, J. et al.: Energy-flux relationship in the FUV Jovian aurora deduced from HST-STIS spectral observations, *J. Geophys. Res.*, 109, A10205, doi:10.1029/2003JA010365, 2004.
- [2] Yoshikawa, I. et al.: Extreme ultraviolet radiation measurement for planetary atmospheres/magnetospheres from the earth-orbiting spacecraft (EXCEED), *Space Sci. Rev.*, 184, 237–258, DOI:10.1007/s11214-014-0077-z, 2014.
- [3] Kimura, T. et al.: Transient internally driven aurora at Jupiter discovered by Hisaki and the Hubble Space Telescope, *Geophys. Res. Lett.*, 42, doi:10.1002/2015GL063272, 2015.
- [4] Tao, C. et al.: Magnetic field variations in the Jovian magnetotail induced by solar wind dynamic pressure enhancements, *J. Geophys. Res.*, 110, A11208, doi:10.1029/2004JA010959, 2005.
- [5] Shiota, D. et al.: Inner heliosphere MHD modeling system applicable to space weather forecasting for the other planets, *Space Weather*, 12, doi:10.1002/2013SW000989, 2014.
- [6] Tao, C. et al.: Variation of Jupiter's Aurora Observed by Hisaki/EXCEED: 1&2, submitted to JGR.



# Simulations of the auroral signatures of Jupiter's magnetospheric injections

**M. Dumont** (1), D. Grodent (1), A. Radioti(1), B. Bonfond(1), E. Roussos(2) and C. Paranicas(3)

(1) Laboratory for Planetary and Atmospheric Physics, university of Liège, Belgium, (2) Max Planck Institute for Solar System Research, Göttingen, Germany (3) Applied Physics Lab, Johns Hopkins University, Laurel, United States  
(maite.dumont@ulg.ac.be / Fax: +32-43669711)

## Abstract

We report the evolution of ultraviolet auroral features located equatorward of the main emission appearing in the Hubble Space Telescope (HST) images of the northern and the southern Jovian hemisphere. We investigate the possibility that those ultraviolet auroral structures are associated with energetic particle injections. For this study, we compare the characteristics of the simulated auroral signature of plasma injections with the observed parameters of equatorward isolated auroral structures.

## 1. Introduction

Jupiter's ultraviolet auroral emissions are divided into four main components: the polar emissions, the main emission, the satellite footprints and the outer emissions. The morphology of the outer emissions can be either diffuse, arc-shaped or compact emissions. In the present study, we focus on outer emissions clearly detaching from the main emission and forming compact structures that are evolving regardless of the rest of the auroral emission. These auroral features were selected because they have the same appearance as the auroral signature of a clearly identified injection previously observed by Mauk et al. [2002] at Jupiter, based on simultaneous Galileo spacecraft and Hubble Space Telescope measurements.

### 1.1 Plasma injections

Mauk et al. [1997] reported the first detection of energetic particle injection in Jupiter observed with the Energetic Particles Detector (EPD) on board the Galileo spacecraft. During a plasma injection, the magnetic flux lost through cold plasma outflow is balanced by inward injection of flux tubes containing hot plasma from the outer magnetosphere. Mauk et al. [1999] performed a statistical analysis of these

energy-time dispersed intensifications in energetic ions and electrons, based on Galileo EPD data, and found that energetic particle injections are commonly observed in the Jovian magnetosphere. Later on, Mauk et al. [2002] associated an isolated equatorward patchy auroral ultraviolet emission with energetic particle injections threading the same flux tube. Nevertheless this association is based on a single set of simultaneous observations.

The goal of the present study is to simulate the auroral signatures of plasma injections by considering that the precipitating energy could be provided to the ionosphere by pitch angle diffusion and whistler-mode waves through electron scattering. We use the concept of simulation described in Radioti et al. [2013]. We compare the length and the brightness of the simulated signature with the observed parameters. Following this comparison, we are able to test whether the aforementioned mechanism is responsible for the auroral emission and to infer the typical energy and the spectral index of the energy distribution of the electrons involved in the injection process.

## 2. Equatorward isolated auroral structures

The equatorward isolated auroral features (Figure 1) consist of quasi-corotating isolated structures spanning a region roughly bounded poleward by Jupiter's main emission, and equatorward by the magnetic footpath of Io.

Dumont et al. [2014] reported the first statistical study of Jovian auroral features possibly associated with signatures of magnetospheric injections. The authors examined the possibility that the selected UV auroral features are related to injection events in the Jovian magnetosphere, they statistically investigated the properties of the equatorward auroral emissions.

They demonstrated that the features studied and energetic particles injection measurements from Galileo spacecraft are present at the same location in the magnetosphere, indicating that the auroral features under study are most probably signatures of injections.

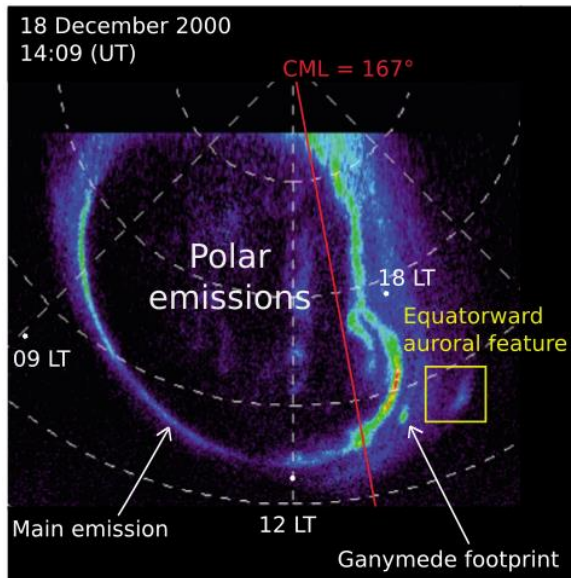


Figure 1: Polar projection of an HST/STIS image in a reference frame fixed in System III. The image shows the northern Jovian aurora on 18 December 2000 at 14:09 UT. The central meridian longitude (red line) is  $167^\circ$  System III. In this particular case, noon (12 LT) is approximately toward the bottom and dusk (18 LT) to the right. The main auroral features are indicated: the main emission, Ganymede footprint, polar emissions, and equatorward auroral feature.

### 3. Summary and Conclusions

In this study, we simulate the auroral signatures of plasma injections and we compare the characteristics of the simulated signature with the observed parameters. We analyze the temporal variations of the longitudinal extent and of the brightness of the auroral structures. Indeed, the injected charged particles drift at different rates due to energy-dependent gradient and curvature drifts, which leads to an increase with time of the longitudinal extent of the feature and of its associated auroral signature. Since the injected energy follows the same trend, the brightness decreases with time.

Different processes can generate auroral signatures of plasma injections. We simulate them by considering that pitch angle diffusion is generated by the precipitating energy flux in the ionosphere and whistler-mode waves through electron scattering. We compare the characteristics of the simulated signature with the observed parameters. Following this comparison, we are able to test whether the aforementioned mechanism is responsible for the auroral emission and to infer the typical energy and the spectral index of the energy distribution of the electrons involved in the injection process.

### References

- [1] Dumont, M., Grodent, D., Radioti, A., Bonfond B. and Gérard, J.-C. : Jupiter equatorward auroral features: Possible signatures of magnetospheric injections, *Journal of Geophysical Research: Space Physics*, Vol. 119, pp. 10.068-10.077, 2014.
- [2] Mauk, B. H., Williams, D. J. and McEntire, R. W.: Energy-Time Dispersed Charged Particle Signatures of Dynamic Injections in Jupiter's Inner Magnetosphere. *Geophysical Research Letters*, Vol. 24, pp. 2949-2952, 1997.
- [3] Mauk, B. H., Williams, D. J., McEntire, R. W., Khurana, K. K. and Roederer J. G. : Storm-Like Dynamics of Jupiter's Inner and Middle Magnetosphere. *Journal of Geophysical Research*, Vol. 104, pp. 22759-22778, 1999.
- [4] Mauk, B. H., Clarke, J. T., Grodent, D., Watte, Jr, J. H., Paranicas, C. P. and Williams, D. J. : Transient Aurora on Jupiter from Injections of Magnetospheric Electrons. *Nature*, Vol. 415, pp 1003-1005, 2002.
- [5] Radioti, A., Roussos, E., Grodent, D., Gérard, J.-C., Krupp, N., Mitchell, D.G., Gustin, J., Bonfond, B. and Pryor, W. : Signatures of magnetospheric injections in Saturn's aurora, *Journal of Geophysical Research*, Vol. 118, pp. 1922-1933, 2013.

## Dynamics of the active region in Jupiter's aurorae

**B. Bonfond** (1), D. Grodent (1), S. Badman (2), Jean-Claude Gérard (1), Aikaterini Radioti (1), Jacques Gustin (1) and T. Kimura (3), the HST GO12883 and GO13035 teams

(1) LPAP, Université de Liège, Belgium, (2) Lancaster University, United Kingdom, (3) Tamagawa High Energy Astrophysics Laboratory, RIKKEN, Japan (b.bonfond@ulg.ac.be)

### Abstract

The Far-UV aurorae at Jupiter vary on a wide range of timescales. This study focusses on the dynamics of the active region on timescales of a few minutes. Up to now, only the time-tag mode of the Space Telescope Imaging Spectrograph provides access to such fast variations with a high spatial resolution. This active region, located on the dusk flank of the area inside the main auroral oval, is the locus of particularly bright (up to several mega Reyleighs) and sudden (a few tens of seconds) enhancements called flares [1]. A previous study also showed that these flares could re-occur quasi-periodically every 2-3 minutes and propagate from dusk to dawn [2].

Here we use data obtained in 2013 and 2014 to show that this quasi-periodic behaviour is only present on half of the cases and that the affected region could either cover the whole active region or a much smaller area ( $\sim 5000\text{km}^2$ ). We also found areas that were still during part of the observation sequence and then began to blink (see Figure 1). We also show that there is no systematically preferred propagation direction. Finally, sequences acquired successively in the two hemispheres show that the quasi-periodic flares can be in phase.

### References

- [1] Waite, H. et al.: An auroral flare at Jupiter, *Nature*, 410, 2001.
- [2] Bonfond, B., Vogt, M. F., Gérard, J.-C., Grodent, D., Radioti, A. and Coumans, V.: Quasi-periodic polar flares at Jupiter: A signature of pulsed dayside reconnections?, *Geophys. Res. Lett.*, 38, 2011.

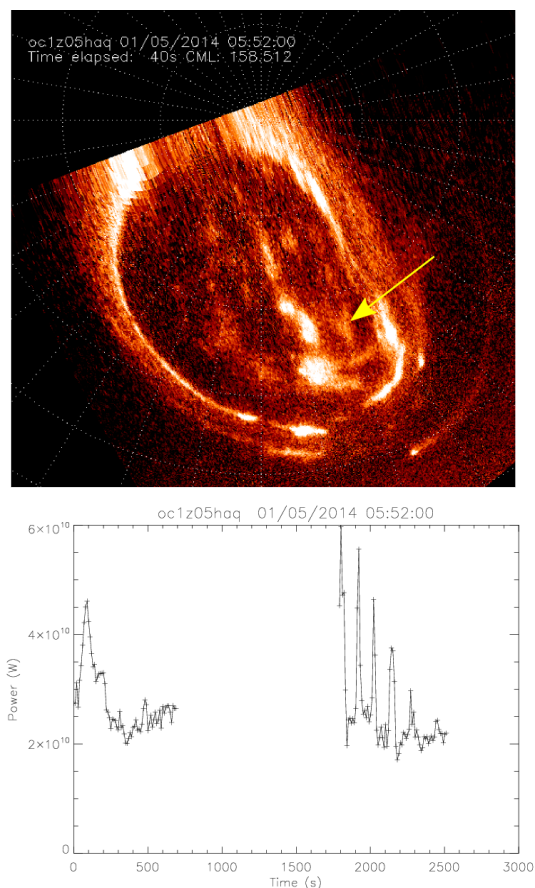


Figure 1: Polar projection of the northern aurorae at Jupiter observed by the Hubble Space Telescope STIS instrument in the Far-UV on January 5th 2014. The bottom plot shows the integrated emitted power for the small V-shaped feature indicated with the arrow. It can be seen that the feature dimmed and then stood still during the first half of the sequence before it began to blink every  $\sim 2.5$  minutes.

## **Statistical analysis of post-equinoctial Uranus' aurorae and implications on the role of solar wind**

L. Lamy (1) and the team of HST GO program #14036  
(1) LESIA, Observatoire de Paris-CNRS, Meudon, France (laurent.lamy@obspm.fr)

### **Abstract**

The re-detection of Uranian Ultraviolet aurorae with the Hubble Space Telescope in 2011, 4 years after equinox, during active solar wind conditions provided a novel opportunity to study the Uranus' asymmetrical magnetosphere and its interaction with the solar wind over the Uranian revolution around the sun. The identified signatures were tentatively attributed to intermittent magnetic reconnexion with the interplanetary magnetic field. I will present more recent HST observations obtained in 2012 and 2014 with variable solar wind conditions. They revealed additional detections which, in turn, seem to indicate a prominent role of the solar wind in driving auroral precipitations

# Updated modeling of Io and non-Io Radio Auroral Emissions of Jupiter

C. Louis <sup>(1)</sup>, L. Lamy <sup>(1)</sup>, P. Zarka <sup>(1)</sup>, B. Cecconi <sup>(1)</sup> and S. Hess <sup>(2)</sup>

<sup>(1)</sup> LESIA, Observatoire de Paris CNRS, UPMC, Univ. Paris 7, 5 Place Jules Janssen, F-92190 Meudon, France

<sup>(2)</sup> Department of Space Environment, ONERA - The French Aerospace Lab, France

## Abstract

The radio auroral emissions produced by the Jupiter's magnetosphere between a few kHz and 40MHz, the most intense of our Solar System, are known since half a century, but they still drive many questions, and their deepened study is one of the main aim of the JUNO missions (arrival in July 2016). Jovian auroral radio emissions are thought to be produced through the Cyclotron Maser Instability (CMI), from non-maxwellian weakly relativistic electrons gyrating along high-latitude magnetic fields lines (Zarka, 1998). These emissions divide in different spectral components, driven or not by the moon Io. The origin and the relationship between kilometric, hectometric and decametric non-Io emissions in particular remains poorly understood.

To investigate these emissions, we simulated numerical dynamic spectra with the most recent version of the ExPRES code - Exoplanetary and Planetary Radio Emission Simulator, available at <http://maser.obspm.fr> - already used to successfully model Io decametric and Saturn's kilometric arc-shaped emissions (Hess et al., 2008, Lamy et al., 2008) and predict exoplanetary radio emissions (Hess et al., 2011). Such simulations bring direct constraints on the locus of active magnetic field lines and on the nature of CMI-unstable electrons (Hess et al., submitted). We validated the new theoretical calculation of the beaming angle used by ExPRES, which now includes refraction at the source. We then built updated simulations of Io and non-Io emissions which were compared to the radio observations acquired by the Cassini spacecraft (Jupiter flyby in 2000) and the Nançay decameter array (routines observations of Jupiter).

## 1. Figure

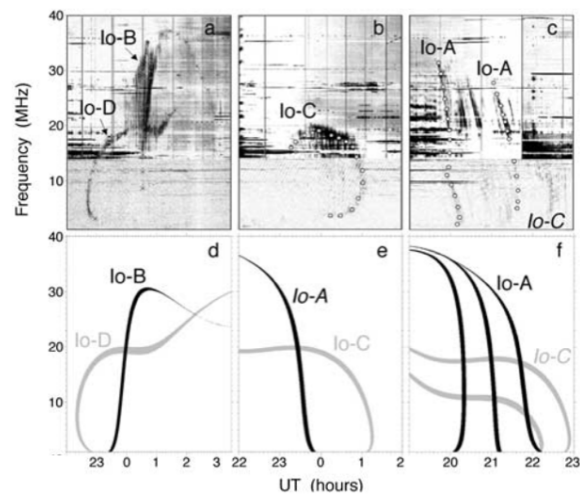


Figure 1: (a, b, c) Dynamic spectra of typical Io-Jupiter arcs observed by Wind/Waves and the Nançay decameter array. (d, e, f) Dynamic spectra of Io-Jupiter emissions for the same t-f intervals as in Figures 3a, 3b, and 3c, simulated by the ExPRES code using actual observing geometries (Black arcs are generated in the northern hemisphere and grey in the southern one. Labels in italics indicate weak or unobserved arcs).

## References

- [1] Zarka, P. (1998), Auroral radio emissions at the outer planets, *Journal of geophysical research*, VOL. 103, NO. E9, PAGES 20,159-20,194, August 30, 1998
- [2] Hess, S., B. Cecconi, and P. Zarka (2008), Modeling of Io-Jupiter decameter arcs, emission beaming and energy source, *Geophys. Res. Lett.*, 35, L13107, doi:10.1029/2008GL033656.
- [3] Lamy, L., P. Zarka, B. Cecconi, S. Hess, and R. Prange (2008), Modeling of Saturn kilometric radiation arcs and equatorial shadow zone, *J. Geophys. Res.*, 113, A10213, doi:10.1029/2008JA013464.
- [4] S. L. G. Hess and P. Zarka (2011), Modeling the radio signature of the orbital parameters, rotation, and magnetic field of exoplanets, *A&A* 531, A29, doi:10.1051/0004-6361/201116510.
- [5] S. L. G. Hess, P. Zarka, B. Cecconi, and L. Lamy (submitted), ExPRESS : a tool to simulate planetary and exoplanetary radio emissions, *A&A*



## **JUICE/RPWI/JENRAGE: a low frequency radio imager at Jupiter**

B. Cecconi (1), Y. Kasaba (2), J. Bergman (3), P. Zarka (1), L. Lamy (1), S. L. G. Hess (4), H. Rothkaehl (5)

(1) LESIA, CNRS-Observatoire de Paris, Meudon, France. (2) Tohoku University, Sendai, Japan. (3) IRFU, Uppsala, Sweden. (4) ONERA, Toulouse, France. (5) SRC-PAS, Warsaw, Poland.

Email: [baptiste.cecconi@obspm.fr](mailto:baptiste.cecconi@obspm.fr)

### **Abstract**

The JENRAGE (Jovian Environment Radio Astronomy and Ganymede Exploration) experiment of the Radio and Plasma Waves Instrument (RPWI) on-board JUICE (Jupiter Icy Moon Explorer) is a sensitive, and versatile radio instrument. It will observe radio waves ranging from 80 kHz to 45 MHz at a 100 Msample per second acquisition rate. The instrument is composed of set of 3 electrical dipoles (developed by the Polish team), connected to low noise preamplifiers and conditioning analog filters (built by the Japanese team), then sampled and digitally filtered into ~300 kHz bands (digital part developed by the Swedish team). This international project is coordinated by B. Cecconi and Y. Kasaba, both co-PI of JUICE/RPWI.

Although the radio antenna connected to this instrument have no intrinsic directivity, the JENRAGE measurements can provide instantaneous direction of arrival, flux density and polarization degree of the observed radio waves. Hence, the JENRAGE can be described as an full-sky radio imager. As the instrument provides direction of arrival, radio sources can be located with some assumption on the propagation between the source and the observer. Hence, it is possible to produce radio source maps and correlate them with observations at other wavelengths, such as UV or IR observations of the auroral regions of Jupiter. The flux and polarization measurements together with the time- frequency shape of the radio emissions can also be used to identify the radio emission processes.

These features have shown their capabilities on Cassini, with the RPWS/HFR instrument.

We will present the JUICE/RPWI/JENRAGE design and the science objectives. Additional science topics linked to the icy satellites, which are currently being assessed, will also be presented.

# The APIS service : a tool for accessing value-added HST planetary auroral observations over 1997-2015

L. Lamy (1), F. Henry (1), R. Prangé (1) and P. Le Sidaner (2)

(1) LESIA, Observatoire de Paris-CNRS, Meudon, France (laurent.lamy@obspm.fr), (2) Observatoire de Paris, Paris, France.

## Abstract

The Auroral Planetary Imaging and Spectroscopy (APIS) service <http://obspm.fr/apis/> provides an open and interactive access to processed auroral observations of the outer planets and their satellites. Such observations are of interest for a wide community at the interface between planetology, magnetospheric and heliospheric physics. APIS consists of (i) a high level database, built from planetary auroral observations acquired by the Hubble Space Telescope (HST) since 1997 with its mostly used Far-Ultraviolet spectro- imagers, (ii) a dedicated search interface aimed at browsing efficiently this database through relevant conditional search criteria (Figure 1) and (iii) the ability to interactively work with the data online through plotting tools developed by the Virtual Observatory (VO) community, such as Aladin and Specview. This service is VO compliant and can therefore also been queried by external search tools of the VO community. The diversity of available data and the capability to sort them out by relevant physical criteria shall in particular facilitate statistical studies, on long-term scales and/or multi-instrumental multi-spectral combined analysis [1,2]. We will present the updated capabilities of APIS with several examples. Several tutorials are available online.

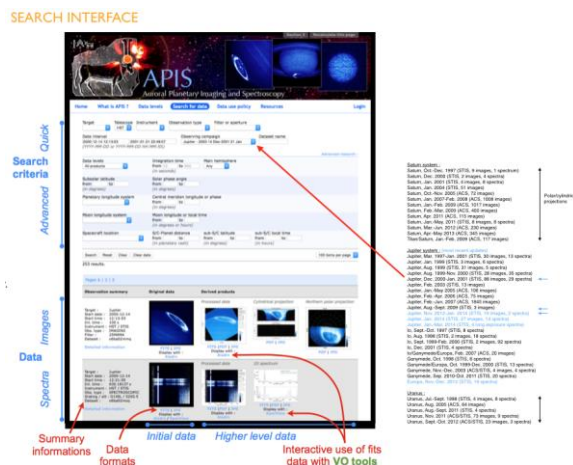


Figure 1 : Search interface. Example of Jupiter data request

## References

- [1] L. Lamy, R. Prangé, F. Henry, P. Le Sidaner, The Auroral Planetary Imaging and Spectroscopy Service (APIS), *Astronomy and Computing*, 11, B, 138-145, Jun. 2015.
- [2] W. S. Kurth, G. Hospodarsky, D. Gurnett, L. Lamy, M. Dougherty, J. Nichols, E. Bunce, W. Pryor, K. Baines, U. Dyudina, T. Stallard, H. Melin, F. Crary, Saturn Kilometric Radiation intensities during the Saturn auroral campaign of 2013, *Icarus*, in press.